

Phonon Dispersion of an Epitaxial Monolayer Film of Hexagonal Boron Nitride on Ni(111)

E. Rokuta, Y. Hasegawa, K. Suzuki, Y. Gamou, and C. Oshima

Department of Applied Physics, Waseda University, 3-4-1 Okubo, Shinjuku-ku, Tokyo 169, Japan

A. Nagashima

Department of Physics, Tokyo Institute of Technology, Ookayama, Meguro-ku, Tokyo 152, Japan

(Received 9 June 1997)

Phonon spectra for epitaxial monolayer films of *hexagonal* boron nitride (*h*-BN) on Ni, Pd, and Pt (111) have been measured for the first time by using high resolution electron energy loss spectroscopy. On Ni(111), we have found two remarkable features in the observed dispersion curves: a level splitting at the crossing point of two phonon branches and degeneracy of two optical phonons with in-plane polarization at $\bar{\Gamma}$, which means the rumpled structure of the *h*-BN film and the elimination of electric fields parallel to the film, respectively. [S0031-9007(97)04733-9]

PACS numbers: 63.20.Kr, 68.35.Bs, 68.35.Ja, 82.80.Pv

Recently, new types of compounds including π electrons have intrigued fundamental explorations in material science, because of their peculiar atomic structure, and their characteristic physical properties; for instance, they are fullerenes [1], nanotube [2], and one sheet of graphite, *hexagonal* boron nitride (*h*-BN) [3], and BNC₂ compounds [4]. *h*-BN is a typical insulating layered material with strongly anisotropic chemical bonds similar to graphite. The basal (0001) plane grows preferentially on various solid surfaces either in a commensurate manner as on Ni(111) or in an incommensurate manner on other surfaces such as Pd, Pt, and TaC (111) [3,5]. Recent studies on the electronic band structures of the monolayer *h*-BN films clarified the peculiar interfacial bonds, weak bonds for the incommensurate systems, and relatively strong bonds for the commensurate system [5]. Most of the observed energy levels and bands referred from the vacuum level agreed perfectly with each other, which is a characteristic of a physisorbed rare-gas solid on various substrates [6]. An exception was the π band of the monolayer *h*-BN film on Ni(111), which has a deeper binding energy by 1 eV than those of the other films [5].

In this Letter, we report the first phonon spectra of these *h*-BN films and compare them with bulk data. Being consistent with the metallic nature of *h*-BN in the recent calculations, the phonon dispersion of a monolayer *h*-BN film on Ni(111) exhibits anomalous features differing from those of the *h*-BN films physisorbed on Pd and Pt (111). The facts indicate a rumpled structure of the BN film, and elimination of the electric fields parallel to the film by the screening effect of free electrons. The rumpled structure of the commensurate *h*-BN/Ni(111) has also been confirmed with low-energy electron diffraction (LEED) intensity analysis in this work.

The phonon spectra were measured in an ultrahigh vacuum (UHV) of 1×10^{-8} Pa with a high resolution electron energy loss (HREEL) spectrometer, of which the energy resolution was 1.2 meV (FWHM) for the direct-

through mode [7]. The monolayer *h*-BN films observed in this experiment were prepared on Ni, Pd, and Pt by a surface catalytic reaction of dehydrogenation of borazine molecules (B₃N₃H₆) described in previous papers [3,5]. These BN films show either sharp fundamental LEED spots of the commensurate 1×1 system on Ni(111) or many LEED spots including satellite ones reflected from the incommensurate systems. The monolayer thickness of the films was precisely controlled for all of the cases by adjusting the reaction time, because the surface activity for dehydrogenation is drastically reduced by the *h*-BN formation. The LEED intensities of the commensurate system were measured in another LEED-UHV chamber and the surface atomic structure has been analyzed from the data.

Figure 1 shows typical specular HREEL spectra measured for the monolayer *h*-BN (0001) on all of the three surfaces. The large peak around 91–100 meV in each spectrum originates from the transverse optical (TO) phonon with out-of-plane polarization, TO_⊥ phonon. In the higher energy region from 170 to 200 meV, on the other hand, small peaks appear; there are three on Pd and Pt, and only one on Ni in Fig. 1. From their energy and intensity, the highest peak was assigned to the second harmonic of the TO_⊥ phonon. The remaining two loss peaks just below the second harmonics on Pd and Pt are attributed to the phonons with in-plane polarization; the higher energy peak originates from the longitudinal optical (LO) phonon, and the lower one from the transverse optical phonon with in-plane polarization, TO_∥ phonon. It should be noted that no LO or TO_∥ phonons were detected for *h*-BN/Ni(111), which means that the parallel fields accompanied with phonon excitations are completely shielded there. In Table I, these phonon energies at $\bar{\Gamma}$ of the two-dimensional Brillouin zone (2D BZ) are tabulated. The vibrational energies of the LO and TO_∥ phonons on Ni are obtained only in the off-specular spectra discussed in the next section.

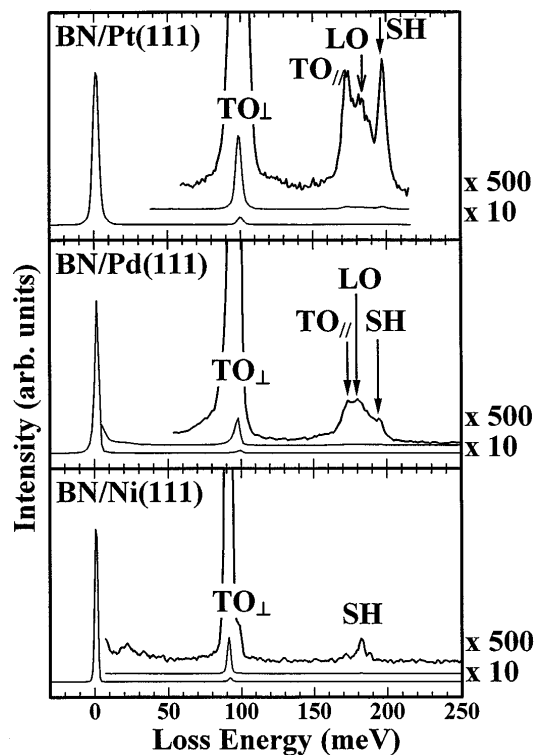


FIG. 1. Typical specular HREEL spectra of monolayer h -BN films on Ni, Pd, and Pt (111). The large peaks at 90–100 meV are attributed to the TO_{\perp} phonons with out-of-plane polarization to the basal plane. Small peaks located at 180–200 meV originated from the second harmonic peak of the TO_{\perp} phonon, and the LO and TO_{\parallel} phonons with the in-plane polarization. The second harmonic peaks are indicated by SH. The spectra are measured with an energy resolution of 2–3 meV.

When we change the scattering geometry from the specular to the off-specular condition, both loss energies and peak intensities change drastically [8]. The wave vectors q_{\parallel} of the observed phonons are changed in accord with the law of conservation of momentum parallel to the surface. The plots of the loss energies against q_{\parallel} provide the energy dispersion curves. The energy and wave vector (momentum) resolutions in this measurement were ~ 1 meV and ~ 0.004 nm $^{-1}$, respectively. Figure 2

shows the experimental curves along $\overline{\Gamma K}$ in the 2D BZ of monolayer h -BN/Ni(111). The data points are indicated by open circles. In Fig. 2, we observed several phonon branches, of which most of the vibrational amplitude is strongly localized in the h -BN film. The optical branch with a flat dispersion curve around 20 meV is attributed to the mode in which the whole h -BN overlayer vibrates against the substrate at $\overline{\Gamma}$. Unfortunately, because of the relatively poor crystalline quality of the films on Pd and Pt (111), phonon dispersion curves of the films on Pd and Pt (111) were not clearly observed as compared with the Ni(111) case.

For comparison, the corresponding bulk data [9] at $\overline{\Gamma}$ are illustrated by four arrows in Fig. 2, and tabulated in Table I. Since a unit cell of the bulk h -BN crystal includes two basal layers, each of these optical phonons consists of two modes. The energies of the LO and TO_{\parallel} phonons of the monolayer h -BN/Ni(111) at $\overline{\Gamma}$ are obtained by extrapolating these curves to $\overline{\Gamma}$ in Fig. 2.

In Table I, roughly speaking, the energies of the transverse phonons are in accord with the bulk ones; all of the observed TO_{\parallel} energies are either very close to the bulk ones or slightly large. Owing to the shielding of the long-range Coulomb interaction by free electrons, however, all of the observed LO phonons show lower energies than the bulk one; by 17 meV on Pt, 21 meV on Pd, and 30 meV on Ni. In particular, it should be noted that the LO phonon is degenerate with the TO_{\parallel} phonon on Ni, which will be discussed later. Concerning the phonon energies, therefore, the properties of the BN film on Pt resemble those of the bulk h -BN crystal, but a large discrepancy was found in the film on Ni.

In Fig. 2 we have found a remarkable feature, the level splitting at the crossing point of the TO_{\perp} and LA branches on the $\overline{\Gamma K}$ axis, as also illustrated by the inset in Fig. 2. This is in contrast to monolayer graphite (MG) on various surfaces, and no similar splitting was observed in the phonon dispersion in MG [10]. Lattice dynamical calculations based on a force constant model indicate a ruffled basal plane; the observed splitting cannot be expected for a flat basal plane, because of their orthogonal eigenvectors.

TABLE I. Some data of a bulk h -BN crystal and monolayer h -BN films on three substrates. The observed vibrational energies of optical phonons at $\overline{\Gamma}$ are in units of meV, and the work functions with (and without) monolayer h -BN layer are in units of eV. Here, the dielectric constant $\epsilon(\omega)$ was calculated based on the Kramers-Kronig relation from the experimental reflectivity.

System	Interfacial structure	Work functions ^a (eV)	TO_{\perp} (meV)	TO_{\parallel} (meV)	LO (meV)
h -BN/Ni(111)	Commensurate 1×1	3.6 (5.3)	91	170	170
h -BN/Pd(111)	Incommensurate	4.0 (5.3)	98	173	179
h -BN/Pt(111)	Incommensurate	4.9 (5.8)	99	173	183
Bulk h -BN	97, 103	169, 170	200 ^b

^aA. Nagashima *et al.* (Refs. [3,5]).

^bThe frequency of the LO phonon in bulk was estimated by the condition $\epsilon(\omega) = 0$.

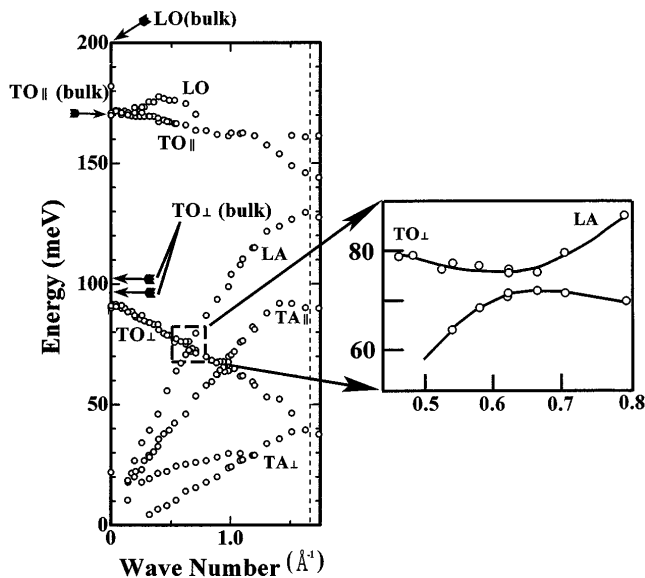


FIG. 2. Phonon dispersion curves of monolayer *h*-BN film on Ni(111). One part around the crossing points of two branches is expanded in the extra figure.

To clarify directly the rumpled structure in the commensurate *h*-BN/Ni(111) system, we have applied LEED intensity analysis. The I-V curves of the (10), (01), and (11) diffraction spots of a 1×1 atomic structure were measured from 100 to 300 eV. A tensor LEED program [11] was used both for evaluating the several surface models meeting the 3 m symmetry of the observed LEED pattern, and for adjusting the atomic positions. Among those models, the most plausible structure exhibiting the lowest "Pendry reliability factor" of $R_p = 0.27$ [12] is depicted in Fig. 3.

We notice some interesting features in this structure. First, the structure is very similar to that of MG/Ni(111) [13]; instead of carbon atoms, boron and nitrogen atoms are situated at the fcc threefold hollow site and atop the site over the outermost Ni atoms, respectively. Second, the interfacial spacing of ~ 0.2 nm is very close to that of MG/Ni and is very narrow in comparison with the bulk interlayer spacing of ~ 0.33 nm. Third, a large difference from the MG is a rumpled structure for the *h*-BN film; the B atoms are situated ~ 0.02 nm below the N atoms. On the contrary, no rumpled structure was detected in MG either from atomic structure analysis [13] or from phonon spectroscopy [10].

Why does the rumpled structure occur only in the *h*-BN film, and not in the MG film? We can find the reasonable explanation based on the lattice mismatch of these materials. Although the in-plane lattice constant of bulk graphite is 1.2% smaller than the nearest neighbor Ni-Ni distance on Ni(111), the in-plane lattice constant of the bulk *h*-BN is 0.4% larger. For construction of the observed 1×1 structure on Ni(111), therefore, the MG plane expands by increasing the C-C distance, and, on the other hand, the *h*-BN plane has to shrink either by shortening the B-N distance or by producing a rumpled

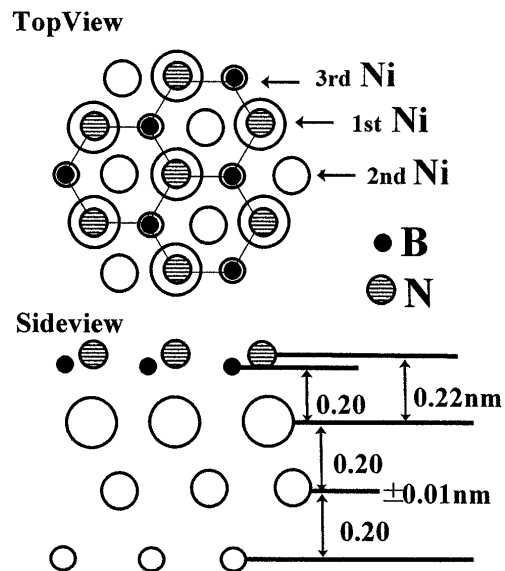


FIG. 3. Atomic structures of the monolayer *h*-BN/Ni(111) system with a commensurate 1×1 periodicity revealed by LEED intensity analysis.

structure; Fig. 3 indicates that the *h*-BN plane shrinks, keeping the B-N distance fixed by introducing the rumpled structure. The observed rumpled structure means that the sp^3 -like bonding character of cubic-BN (*c*-BN) exists partially in the BN bonds of *h*-BN film; the amplitude is one third of the rumpling amplitude of N and B atoms on *c*-BN(111), 0.06 nm. Recently, the preferential growth of *c*-BN films was reported only on the polycrystalline Ni wire by plasma chemical vapor deposition [14]. The correlation with the observed structure is a remaining interesting research subject.

Another remarkable feature in the dispersion curves in Fig. 2 is the degeneracy of the LO and $TO_{||}$ phonons at $\bar{\Gamma}$, which provides splendid information on the interesting nature of the film on Ni. As shown in Table I, the degeneracy was observed only for *h*-BN/Ni(111), not for the other systems. The energy of the LO phonon approaches the bulk one, changing the substrate from Ni to Pt as mentioned before.

According to the lattice dynamical theory based on a shell model, which successfully reproduces the phonon dispersion curves in many ionic materials [15], the $TO_{||}$ phonon energy at $\bar{\Gamma}$ was determined mainly by the short range interactions, and, on the other hand, the LO phonon energy at $\bar{\Gamma}$ by both the short- and the long-range interactions. The LO polarization fields, consequently, generate the level splitting between the LO and $TO_{||}$ phonons at $\bar{\Gamma}$ in normal ionic materials. On the contrary, the degeneracy occurs for nonpolar materials, such as Si, Ge, diamond, and graphite, and the metallic compounds, such as TiC, ZrC, and NbN. In both cases, no LO polarization fields are excited because of either their nonpolar-bonding character or screening by free electrons [16].

The same phenomenon was also noticed in the loss intensity of the specular spectra in Fig. 1. As mentioned

before, both the LO and TO_{\parallel} phonon peaks on Ni are negligible. That is to say, the dipole fields accompanied with these phonon excitations can extend to the vacuum on Pd and Pt, but not on Ni. At first sight, the origin of these two phenomena concerning screening seems to be attributed to the collective motions of free electrons in the substrate. Because of the high frequency of the plasmon and/or surface plasmon, the free electrons in the metallic substrate may possibly shield the parallel components of the dipole electric fields generated by the LO and TO_{\parallel} phonon excitations. From the estimation of the fields on the basis of the image-charge model, however, the observed large difference between Ni and the others cannot be explained. Only from the difference in interfacial spacings, 0.21 nm on Ni in Fig. 3 and much larger on Pd and Pt, for instance, 0.333 nm [17], we cannot explain the observed perfect screening of the parallel fields. Hence, we next consider an additional mechanism for this perfect screening.

Recent theoretical calculations of the bands for the atomic structure in Fig. 3 provide a plausible interpretation for this perfect shielding on Ni [18]; orbital hybridization of π electrons with d electrons of Ni substrate tends to enlarge with decreasing the interfacial spacing below 0.25 nm. For the atomic structure in Fig. 3, as a result, the metallic interfacial bands are caused by the orbital hybridization. In addition, the orbital hybridization explains also the binding energy shifts of π bands observed in the previous angle-resolved ultraviolet photoemission spectroscopy experiment [5]. Therefore, the hybridized π electrons in the BN films participate in eliminating the in-plane electric fields. Since no evidence for orbital hybridization was found on Pd and Pt, only the electrons inside the substrates can move for screening there.

The orbital hybridization is consistent with the other experimental facts: the decrease in the TO_{\perp} and TO_{\parallel} phonon energies on Ni(111) from the bulk values and the relatively low work function of h -BN covered Ni(111) in Table I.

In summary, we found a novel system of monolayer h -BN on Ni(111), of which properties are much different from those of the bulk h -BN. The monolayer h -BN film/Ni(111) overcomes the lattice mismatch problem by introducing ruffled structure, which results in the formation of the commensurate 1×1 system. The orbital hybridization at the narrow interface produces the metallic bands, which enable the π electrons to participate in the

elimination of the LO polarization parallel to the surface and the parallel dipole fields accompanied with LO or TO_{\parallel} phonon excitations.

-
- [1] H. W. Kroto, J. R. Heath, S. C. O'Brien, and R. E. Smalley, *Nature* (London) **318**, 162 (1985).
 - [2] S. Iijima, *Nature* (London) **354**, 56 (1991).
 - [3] C. Oshima and A. Nagashima, *J. Phys. Condens. Matter* **9**, 1 (1997).
 - [4] M. O. Watanabe, S. Itoh, T. Sasaki, and K. Mizushima, *Phys. Rev. Lett.* **77**, 187 (1996); see also, M. Kawaguchi and N. Barlett, *Fluorine-Carbon and Fluoride-Carbon Materials*, edited by T. Nakajima (Marcel Dekker, Inc., New York, 1995), Chap. 5, p. 187.
 - [5] A. Nagashima, N. Tejima, Y. Gamou, T. Kawai, and C. Oshima, *Phys. Rev. Lett.* **75**, 3918 (1995); *Phys. Rev. B* **51**, 4606 (1995); A. Nagashima, N. Tejima, Y. Gamou, T. Kawai, M. Terai, M. Wakabayashi, and C. Oshima, *Int. J. Mod. Phys. B* **10**, 3517 (1996).
 - [6] K. Jacobi, *Surf. Sci.* **192**, 499 (1987).
 - [7] T. Nagao, Y. Iizuka, M. Umeuchi, T. Shimazaki, and C. Oshima, *Rev. Sci. Instrum.* **65**, 515 (1994).
 - [8] The off-specular spectra were measured by changing the incident angle from 72° to 36° referred to the surface normal, while the reflection angle of 72° is fixed referred to the surface normal. Primary energies used in this measurement were 4–41 eV.
 - [9] R. Geick, C. H. Perry, and G. Rupprecht, *Phys. Rev.* **146**, 543 (1966).
 - [10] T. Aizawa, R. Souda, S. Otani, Y. Ishizawa, and C. Oshima, *Phys. Rev. B* **42**, 11 469 (1990).
 - [11] P. J. Rous, M. A. Van Hove, and G. A. Somorjai, *Surf. Sci.* **226**, 15 (1990).
 - [12] Y. Gamou, M. Terai, A. Nagashima, and C. Oshima, *Sci. Rep. Res. Inst. Tohoku Univ. A* **44**, 211 (1997).
 - [13] Y. Gamou, A. Nagashima, M. Wakabayashi, M. Terai, and C. Oshima, *Surf. Sci.* **374**, 61 (1997).
 - [14] F. Zhang, Y. Guo, Z. Song, and G. Chen, *Appl. Phys. Lett.* **65**, 971 (1994).
 - [15] P. Bruesch, *Phonons: Theory and Experiments I* (Springer-Verlag, Berlin, 1982).
 - [16] H. Bilz and W. Kress, *Phonon Dispersion Relations in Insulators* (Springer-Verlag, Berlin, 1979).
 - [17] So far, there is no data about the interfacial spacing of h -BN/Pd (and Pt). If we assume the 0.33 nm because of the physisorption, we can estimate the 10% reduction.
 - [18] T. Kawai, Y. Souzu, T. Osaka, T. Tsukada, and C. Oshima (unpublished).